THE EFFECT OF IRON CONTENT ON THE PHASE TRANSFORMATION OF TIO_2 NANOCRISTALLINE POWDERS PREPARED BY SOL GEL PROCESS

Reçu le 11/05/2009 – Accepté le 23/11/2010

Résumé

Les nanoparticules de TiO_2 pure et dopé par des ions +3 de fer (Fe^{+3}) ont été préparées par la méthode Sol -gel, utilisant le $TiCl_4$ et le $FeCl_3$ comme des précurseurs, l'éthanol comme un solvant et l'hydroxyde d'ammonium comme un catalyseur. Les propriétés structurelles, morphologiques et optiques des poudres préparées ont été examinées par la diffraction des rayons X (DRX), la microscopie électronique à balayage (MEB) et la spectroscopie d'absorption UV-visible. La qualité des échantillons a été examinée par la spectroscopie Infrarouge (IR) et la photoluminescence à température ambiante (PL). Tous les échantillons cristallisent sous la phase anatase sauf l'échantillon dopé a 0.1 % mol, ou la phase rutile a été apparue. Les tailles de particules diminuent quand le pourcentage du fer augmente dans les échantillons. Les images du MEB montrent que la morphologie et la taille des particules sont affectées par la quantité du dopant. La limite d'absorption des échantillons (TiO_2 dopés Fe^{3+}) se déplacée vers le spectre visible quand la concentration du fer augmente. Les spectres d'absorptions infrarouges, montrent que les échantillons préparés sont purs et possèdent des surfaces fortement hydratées.

Mots-clés: *D*ioxide de titane **;** Sol-gel ; dopage par les ions de fer ; Anatase ; rutile, transformation de phase.

S. BOUDJADAR*
S. MAHMOUDI*
L. GUERBOUS**

*Ceramics laboratory, department of physics, Mentouri University, Constantine, Algeria.

**Department of laser, Nuclear research center, Algiers (CRNA), Algeria.

Abstract

Pure and Fe^{3+} - doped TiO_2 nanoparticles were prepared by sol–gel method, using $TiCl_4$ and $FeCl_3$ as starting materials, ethanol as a solvent and ammonium hydroxide as a catalyst. The structural, morphological and optical properties of as prepared powders were investigated by X-ray diffraction, scanning electron microscopy and UV-visible absorption spectroscopy. The quality of the samples was examined by Infra-red absorption spectroscopy and room temperature photoluminescence (PL). All samples shows anatase phase except the 0.1 mol % Fe^{3+} - doped TiO_2 sample, which rutile phase was appeared. The particle sizes decrease when the iron content increases. From SEM images, the morphology and size of particles were affected by amount of doped metal. The absorption edge of Fe^{3+} - doped TiO_2 shifted towards visible spectrum when the Fe^{3+} - doped concentration increased. from the infra-red absorption spectra, the materials showed a highly pure and strongly surface hydrated, the materials shows main PL emission peaks appears in UV, and visible regions.

Keywords: Titanium dioxide; Sol-gel; Iron ion doping; Anatase; rutile; phase transformation.

ملخص

تم تحضير حبيبات نانومترية لثاني أكسيد التيتان TiO_2 المطعم بالحديد الثلاثي Fe^{+3} بتقنية الصول -جيل، إنطلاقا من $TiCl_4$ و $FeCl_3$ كمصدرين للمادة المحضرة، الإيثانول كمذيب و هيدروكسيد الأمنيوم NH_4-OH كمحفز. أمتحنت الخصائص البنيوية و المورفولوجية و الضوئية للعينات بتقنيات: إنكسار الأشعة السينية DRX، الماسح الإلكتروني SEM، إمتصاصية الأشعة فوق البنفسجية و المرئيةUv-Visible و امتصاصية الأشعة تحت الحمراء Infra-red مع المطيافية الضيائية Photoluminescene. كل العيينات تبارت تحت الطور أناتاز Anatase ماعدا العينة المطعمة ب $0.1\%\ Fe^{+3}$ تبارت تحت الطور ريتيل Rutile . لوحظ انخفاض حجم الحبيبات البلورية مع ارتفاع نسبة التطعيم. توضح صور الماسح الإلكتروني تأثر شكل و حجم الحبيبات مع التطعيم. تبين إمتصاصية الأشعة فوق البنفسجية إنزياح عتبة الإمتصاص باتجاه الطيف المرئي مع ازياد نسبة التطعيم. أما مطيافية الأشعة تحت الحمراء فتوضح بجلاء نقاوة المادة من جهة و شراهتها لإمتصاص الماء من جهة أخرى. المطيافية الضيائية توضح ظهور بعض القمم في منطقة الأشعة فوق البنفسجية و المرئية.

الكلمات المفتاحيـــة: ثنائي أكسيد التيتان، صول-جيل، التطعيم بشوارد الحديد، آناتاز، ريتيل، تحولات الطور.

INTRODUCTION

Titanium dioxide (TiO_2) is one of the most famous semiconducting dioxides, due to its specific properties such as, high photocatalytic activities, transparency in visible region, low cost, non toxicity, easily deposited and easily doped [1 - 3]. However their physical and chemical properties and hence their potential applications depend strongly on their crystalline structure, morphology, particle size and phase composition [4, 5]. It has well been known that the titanium dioxide could be crystallize under three phases, the anatase, rutile and brookite. The anatase phase shows a better photocatalytic activity, the rutile is the thermodynamically most stable phase and the brookite is a high pressure phase. Thus only the anatase and the rutile play a part in the applications of TiO_2. The phase transformation can be affected by several factors like the presence of impurities and doping species, starting materials, synthesis processes, grains size and annealing temperature. Though, there are many contradictory reports concerning the crystallinity and phase transformation in titanium dioxide [6- 9]. Recently, transition metals (Fe, Al, Ni, Co, Mn, Cr, Cu, Zn…) have been used to dope TiO2 in the aim to improve its different properties, particularly crystalline and photocatalytic properties. It has been found, that the addition of small amounts of metal can induce the crystallization of amorphous materials at relatively low annealing temperature [10, 11]. Among transition metals dopants, iron has been considered to be an appropriate candidate because its oxidation state (+3) and its ionic radius (0.79A°) are comparable to those of the titanium (+4 and 0.75 A°). In addition, Fe-doped TiO_2 system is considered as a potential candidate for photocatalyst, and it has reported that the photocatalyst improved with optimal Fe content [12-14]. In the past decade, several techniques have been intensively used to synthesize TiO_2 powders, including sol-gel approach [15 - 17], ultrasonic method [18], hydrothermal technique [19], and solvothermal process [20]. Among these, the sol – gel process is considered an important approach because of its simplicity, less inexpensive and easy to control deposited parameters. Herein, we report the effect of low iron doping concentration on the phase transformation, structural and optical properties and the morphology of TiO_2 nanopowders prepared in one step by sol-gel method at fixed relatively low temperature (350°C), using titanium tetrachloride, iron (III) chloride, ethanol and ammonium hydroxide as a precursor, source dopant solvent and a stabilizer agent respectively. The effect of Fe doping on the crystallization, phase transition and morphology of TiO_2 nanoparticles are studied by X-ray diffraction (XRD), scanning electron microscopy (SEM), UV-visible and FT-IR spectroscopy and photoluminescence (PL) measurement.

2. Experimental

2.1. Preparation of the iron-ion-doped TiO_2

Fe^{3+} - doped TiO_2 nanoparticles were prepared by sol-gel method using titanium tetrachloride ($TiCl_4$) as the source of titanium and iron trichloride ($FeCl_3$) as the source of doping agent. In a typical reaction, 2.5ml of $TiCl_4$ were dissolved in ethanol with a volume ratio of 1:4 under vigorous stirring for 5min in ice water. In the preparation of 0.1 – 1,5 mol % Fe^{3+} -doped TiO_2, the pre-determined amounts of the $FeCl_3$ were added to the previous solution. After the reagents were thoroughly mixed, 0.1M NH_4 – OH (pH=11) solution were added drop by drop under vigorous stirring for 30 min until final pH value of 9. After centrifugal filtration, the powders were dried at 100 C° for 24 h at room temperature, and then calcined under air at 350 C° for 3h.

2.2. Characterization

The phase, the crystalinity and the purity of as prepared Fe^{3+}-doped TiO_2 nanoparticles were determined by X-ray powder diffraction (XRD) in the 20-70°range using Cu kα(λ=1.5406Å) radiation in a Bruker - AXS type D8 diffractometer. The morphology and the size of the particles were observed on VEGA TS 5130 MM scanning electron microscopy (SEM). The UV-visible absorption spectra were obtained in the wavelength range from 200 to 800 nm using an UV-visible spectrophotometer (Shimadzu UV – 2501PC).The composition quality and molecular structure of the synthesized material were characterized, by Fourier transform infrared (FTIR) spectrometer (8201PC, SHIMADZU) in the range (400 – 4000 cm-1) using the KBr pellet technique. The photoluminescence (PL) of Fe-doped TiO_2 powder was investigated at room temperature on Perkin Elmer LS 55 spectrophotometer using 325 nm Xenon laser as the excitation light source.

4. Discussion

4.1. X-ray diffraction

XRD is used to investigate the crystallinity and the phase structure of the samples. Fig. 1 shows the X-ray diffraction patterns of the pure and Fe^{3+} - doped TiO_2 nanoparticles were performed in 2 – theta angular range from 20 to 70 degrees. For undoped and 0.5 to 1.5 mol % Fe^{3+}-doped TiO_2 samples all diffraction peaks obviously correspond to crystalline titanium oxide of anatase phase (JCPDS 78 – 2486). However, it is very surprising that for the sample of 0.1 mol % Fe^{3+} -doped TiO_2, practically all peaks assigned to the rutile phase (JCPDS 78 – 1508), except a very weak peak at 25.3°, which was attributed to the (101) anatase phase peak, indicating that the material mainly crystallize in rutile phase under these conditions. Transition iron oxide phases were not detected in the XRD pattern, suggesting, despite the small amount of dopants, that iron oxide could be existed as the amorphous phase, without incorporating to the TiO_2 lattice or goes to the substitutional sites in TiO_2 lattice, as we mentioned above.

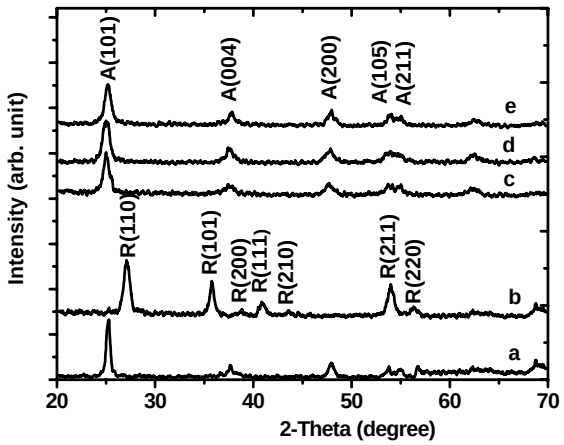

Fig. 1. XRD patterns of pure and Fe^{3+}- doped TiO_2: (a) pure TiO_2, (b) 0.1 %,(c) 0.5%, (d) 1%, (e) 1.5% Fe^{3+}- doped TiO_2.

The average grain size is calculated from the broadening of the (1 0 1) XRD peak of anatase and (110) rutile phases using Scherrer's equation: $D=0.9\lambda/(\beta \cos \theta)$, and the distortion of the TiO_2 matrices was also estimated from the XRD spectra using the formula: $\varepsilon = \beta/4tg\theta$ [21], where λ is the x-ray wavelength (λ=1.5406 Å), θ is the Bragg angle and β is the half-height width of the diffraction peak of anatase and rutile phases. The different characteristics of the studied samples are summarized in Table 1. It can be concluded that doping iron-ion with proper content decreases the crystal size. For example the grain size decrease from 14 nm for the pure TiO_2 to 7.88 nm for 1.5mol % Fe^{3+}-doped TiO_2. The top observation is the appearance of rutile phase at relatively low temperature in 0.1mol % Fe^{3+}-doped TiO_2 sample. It is a surprise to find the appearance of the ritule phase for this amount of doping and at low temperature; it seems that there are other factors except the temperature that they can influence the anatase-ritule phase transformation. As it has been reported [22 - 24] that the phase transformation of anatase to rutile is a surface phenomenon. So this means that the transformation is associated with nucleation on the surface of particles. It is believed that the difference between chemical potential of primary and final phases is the most likely factor which is responsible for activation energy of phase transformation. Nano-particles with small crystallite size have less thermal stability. Therefore, in anatase with smaller particle size it is easier to start the phase transformation at lower temperature than in the large particles under similar condition [25].

4.2. Morphology analysis

Figs. 2 show a typical SEM image of TiO_2 samples synthesized with and without Fe doping. SEM image (Fig. 2a) of the as-prepared TiO_2 shows an ultra-fine powder.

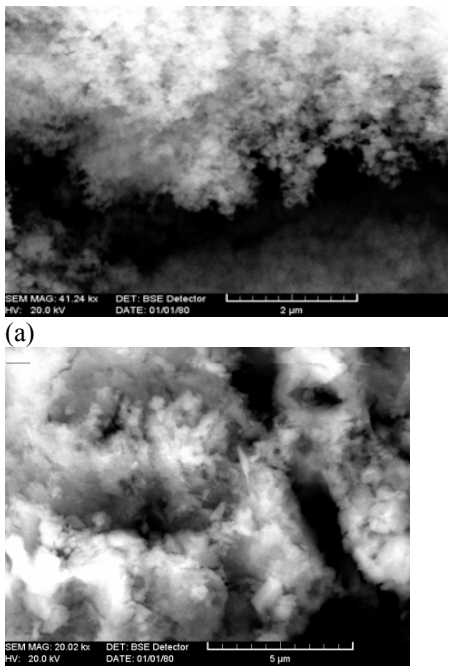

Fig. 2. SEM image of pure and Fe^{3+}- doped TiO_2: (a) pure TiO_2, (b) 0.5% Fe^{3+}- doped TiO_2.

However, the particles in doped samples tend to aggregated together to form bigger particles with various size and shape, the surface of agglomerated particles is rough and compact (Fig. 2b).

4.3. FTIR spectroscopy

IR spectroscopy was used to examine the surface chemical states of the as-prepared sample. FTIR spectra of the TiO_2 and Fe^{3+}-doped TiO_2 are shown in Fig.3. A broad absorption peak at 400–700 cm-1 wavelength ranges is clearly visible. This is attributed to Ti–O stretching and Ti–O–Ti bridging stretching modes [26]. A several absorption bands correspond to the vibrational modes of organic species such as hydroxyl, carboxilate and alkenes groups are observed.

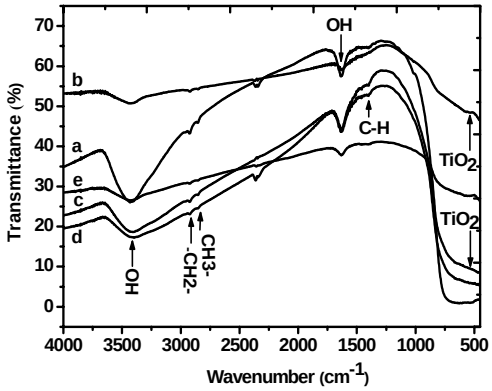

Fig. 3. Infrared spectra of pure and Fe^{3+}- doped TiO_2: (a) pureTiO_2, (b) 0.1 %,(c) 0.5%, (d) 1%, (e) 1.5% Fe^{3+}- doped TiO_2.

A broad band observed between 3700 and 3000 cm-1 and the broad peak at about 1630 cm-1 are related to the O -H stretching mode of hydroxyl groups. [27 - 29]. The peak at 1633 cm-1 in all spectra, is assigned to C–H stretching vibrations of alkenes groups [30]. The weak peaks at about 2850 cm-1 and 2920 cm-1 are normally attributed to the symmetric and to the asymmetric stretching of $–CH_2–$ groups and terminal $CH_3–$ groups [27]. Evidently, the composition of the start materials is the originated of these adsorbed species. These results suggest that the as-prepared TiO_2 nanocrystals are highly pure and strongly surface hydrated, which is significantly different from the water-soluble TiO_2 nanoparticles reported by Wang et al. [31]. In addition the transmittances generally, decrease as doping content increase.

4.4. UV–vis absorption spectra

The UV–vis absorption spectra of TiO_2 and Fe^{3+}- doped TiO_2 prepared by the sol–gel method are shown in Fig. 4. As we can see, the light absorption in the visible range increases with increasing the dopant amount of Fe. The red shift of absorption edge corresponds with a decrease in the band gap. It has been accepted that metal doping could introduce a dopant energy level into the band gap of TiO_2 [32, 33]. A dopant energy level of Fe has also been found to be located close to and above the valence band [33]. Therefore, the red shift of the absorption edge for the Fe^{3+}-doped TiO_2 should come from the electronic transition from the dopant energy level to the conduction band of TiO_2. It has been reported that the shift resulted from the incorporation of iron ions into the TiO_2 nanoparticles prepared by sol–gel method [34, 35]. The red shift in the visible range has a practical importance, since an efficient utilization of visible light for photocatalytic reaction will be possible.

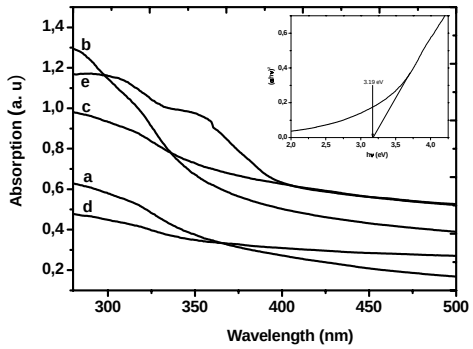

Fig. 4. UV- vis spectra of pure and Fe^{3+} doped TiO_2: (a) pure TiO_2, (b) 0.1 %,(c) 0.5%, (d) 1%, (e) 1.5% Fe^{3+}-doped TiO_2. The insert is the $(\alpha h\upsilon)^2$ versus $h\upsilon$ plot for 0.1% Fe^{3+}-doped TiO_2 sample.

The absorption spectra is extended to the visible range of 400 –500 nm, as a function of iron concentration doping, then show a highly value for 1.5 mol % Fe^{3+}-doped TiO_2 sample. It has been shows a clear reduction in the band gap energy for TiO_2 nanoparticles doped with Fe^{3+} (from 3.17 to 2.75 eV) in comparison with undoped TiO_2 (3.23 eV). XRD and UV–visible studies in combination suggest that Fe^{3+} ions have been incorporated into the lattice of TiO_2 nanoparticles, which is inconsistent with results reported by Wang et al [36]. The relationship of the absorption coefficient and the incident photon energy of semiconductor are given by the following equation [37, 38]:

$$\alpha h\nu = (h\nu - E_g)^n \quad (1)$$

Where α is the absorption coefficient, $h\upsilon$ is the energy of the incident photon, n is 0.5 and 2.0 for a direct transition semiconductor and indirect transition semiconductor respectively. The TiO_2 is a direct gap semiconductor, which has a very small absorption coefficient. The band gaps of various iron ions doping concentration are summarized in Table 1.

Fe (mol %)	Phase	Grain size (nm)	Matrix distortion (%)	E_g (eV)
0	Anatase	14	0.373	3.23
0.1	Rutile	9	0.613	3.19
0.5	Anatase	8.68	0.619	3.02
1	Anatase	8.54	0.621	2.96
1.5	Anatase	7.88	0.674	2.94 2.75

Table 1: Data analysis of pure and Fe^{3+} -doped TiO_2 .

4.5. Photoluminescence spectra

The room temperature photoluminescence (PL) spectra of the specimens are shown in Fig. 5. From the shape and position of the PL emission peaks, there is no evident difference, but their relative intensities exhibit remarkable differences between the undoped TiO_2 and Fe^{3+} doped TiO_2. The PL intensity of the doped TiO_2 is bigger than the undoped TiO_2 in the visible region but generally is lower in UV band. It is well known that PL spectrum of nanostructure materials is related to its transfer behavior of photo-induced electrons and holes, reflecting the separation and recombination of charge carriers [39 – 41]. For the 1.5 mol % Fe^{3+} doped TiO_2 sample, its PL intensity is the weaker among the four doped samples. Thus, recombination rate of charge carriers is the lower. As we can see, at the Fig. 5, the room temperature PL spectra for TiO_2 and Fe^{3+}- doped TiO_2 shows six main emission peaks appear at about 3.23, 3.03, 2.84, 2.78, 2.62 and 2.39 eV, which correspond to the 383, 410, 436, 448, 473 and 518 nm wavelengths respectively. The former is ascribed to the emission of band to band recombination, while the latter is attributed to the electron transition mediated by defect levels such as oxygen vacancies in the band gap [42].

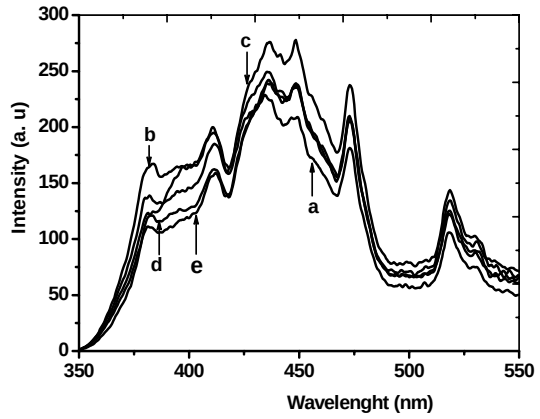

Fig. 5. PL spectra of pure and Fe^{3+}- doped Titania: (a) pureTiO_2, (b) 0.1 %,(c) 0.5%, (d) 1%, (e) 1.5% Fe^{3+}- doped TiO_2.

Compared with the indirect band-gap energy of 3.23 eV obtained by UV–vis absorption measurement, the emission position of the radiative annihilation of excitons exhibited a slight red shift, which is suggested to be related to the light-induced relaxation of polar molecules [43, 44]. The latter is the emission signal originated from the charge-transfer transition from Ti^{3+} to oxygen anionic a TiO_6^{8-} complex [45, 46]. The difference of about 0.84 eV between the band gap energy (3.23 eV) and the emission peak energy (2.39 eV) is caused by the Stokes shift due to the Franck–Condon effect [39, 44].

CONCLUSION

It can be concluded that the weak amounts of iron ion doping can decrease the crystallite size and favorite the Anatase–Rutile transformation at relatively low temperature (350 °C). In this study, the characterization of undoped and Fe^{3+}- doped TiO_2 prepared by a sol–gel method was performed. The particle size and morphology of the Fe^{3+}-doped TiO_2 were strongly dependent on the amount of Fe incorporated in TiO_2 matrix. It can be concluded from the Scherrer equation that doping iron-ion with proper content decreases the crystal size and the anatase to rutile transformation was appeared. The FT-IR analysis suggests that the as-prepared TiO_2 nanocrystals are highly pure and strongly surface hydrated. The undoped TiO_2 sample showed a lowest absorption towards visible light. When doping with iron ions, the absorption spectra are extended to the visible range of 400 –500 nm. UV spectra show a clear reduction in the band gap energy as a function of content doping. PL spectra for TiO_2 and Fe^{3+} doped TiO_2 shows six main emission peaks. The UV band is ascribed to the emission of band to band recombination, while the visible bands are attributed to the electron transition mediated by defect levels such as oxygen vacancies in the band gap. The increase of PL intensity could be attributed to the introduction of new defect sites in the samples. The red shift in the visible range has a practical importance since an efficient utilization of visible light for photocatalytic reaction will be possible.

REFERENCES

[1] Chen X, Mao SS (2007) Chemical Reviews 107: 2891-2959
[2] Andersson M, Osterlund L, Ljungstrom S, Palmavist A (2002) The Journal of Physical Chemistry B 106 (41): 10674-10679
[3] Tada H, Hattori A, Tokihisa Y, Imai K, Tohge N, Ito S (2000) the Journal of Physical Chemistry B 104 (19): 4585–4587
[4] Garcia-Serrano J, Gomez-Hernandez E, Ocampo-Fernandez M, Pal U (2009) Current Applied Physics 9 : 1097–1105
[5] Wang W, Gu B, Liang L, Hamilton WA, Wesolowski DJ (2004) The Journal of Physical Chemistry B 108 (39):14789–14792
[6] Stojanovic B D, Marinkovic Z V, Brankovic G O, Fidancevska E(2000) Journal of Thermal Analysis and Calorimetry 60: 595-604
[7] Gouma P I, Mills MJ (2001) Journal of the American Ceramic Society 84: 619-622
[8] Varghese OK , Gong D, Paulose M, Grimes CA, Dickey EC (2003) Journal of Materials Research 18:156-165
[9] Fernandez-Garcia M, Wang X, Belver C, Hanson JC, Rodriguez JA (2007) The Journal of Physical Chemistry C 111 : 674-682
[10] Izmajlowicz MAT, Flewitt A J, Milne WI, Morrison NA (2003) Journal of Applied Physics 94: 7535-7541
[11] Epifani M, Giannini C, Tapfer L, Vasanelli L (2000) Journal of the American Ceramic Society 83: 2385-2393
[12] Tseng IH, Wu GCS, Chou H (2004) Journal of Catalysis 221: 432-440
[13] Kang M, Mol J (2003) Journal of Molecular Catalysis 197:173-179
[14] Perkas N, Palchik O, Drukental I, Nowik I, Gofer Y, Koltypin Y, Gedanken A (2003) Journal of Physics Chemistry B 107: 8772-8778.
[15] Zhu YF, Zhang L, Wang L, Fu Y, Gao LL (2001) Journal of Materials Chemistry 11: 1864–1868
[16] Zhang L, Zhu Y, He Y, Li W, Sun H (2003) Applied Catalysis B, Environmental 40: 287-292.
[17] Li Z, Shen W, He W, Zu X (2008) Journal of Hazardous Materials 155: 590-594
[18] Peng F, Cai L, Yu H, Wang H, Yang J (2008) Journal of Solid State Chemistry 181: 130–136
[19] Janes R, Knightley LJ, Harding CJ (2004) Dyes Pigments 62: 199–212
[20] Peng F, Cai L, Huang L, Yu H, Wang H (2008) Journal of Physics and Chemistry of Solids 69: 1657–1664
[21] Shi JW, Zheng JT, Hu Y, Zhao YC (2007) Materials Chemistry and Physics 106: 247–249
[22] Moon J, Takagi H, Fujishiro Y, Awano M (2001) Journal of Materials Science 36: 949-955
[23] Ronconi C M, Ribeiro C, Bulhoes LOS, Pereira EC (2008) Journal of Alloys and Compounds 466: 435-438

[24] Li W, Ni C, Lin H, Huang CP, Shah SI (2004) Journal of Applied Physics 96: 6663-6668
[25] Mahshid S, Askari M, Ghamsari M S, Afshar N, Lahuti S (2009) Journal of Alloys and Compounds 478 : 586-589
[26] Peiro AM, Peral J, Domingo C, Momenech X, Ayllon JA (2001) Chemistry of Materials13: 2562-2567.
[27] Sun A, Li Z, Li M, Xu G, Li Y, Cui P (2010) Powder Technology 210 :130-137
[28] T. Bezrodna, G. Puchkovska, V. Shimanovska, I. Chashecnikova, T. Khalyavka, Baran J (2003) Applied Surface Science 214: 222-231
[29] Kanna M, Wongnawa S, Material Chemistry and Physics 110 (2008) 166-175
[30] Li GS, Li LP, Goates JB, Woodfield BF (2005) Journal of the American Chemical Society 127: 8659-8666
[31] Wang P, Wang DJ, Li HY, Xie TF, H. Z. Wang, Z. L. Du (2007) Journal of Colloid and Interface Science 314: 337-340
[32] Cao YA, Yang WS, Zhang WF, Liu GZ, Yue P (2004) New Journal of Chemistry 28: 218–222
[33] Li XZ, Li FB (2001) Environnemental Science and Technology 35 : 2381–2387
[34] Kim DH, Hong HS, Kim SJ, Song JS, Lee KS (2004) Journal of Alloys and Compounds 375: 259–264
[35] Ghorai TK, Biswas S K, Pramanik P (2008) Applied Surface Science 254: 7498-7504
[36] Wang XH, Li JG, Kamiyama H, Katada M, Ohashi N, Moriyoshi Y et al (2005) Journal of American Chemistry society 127: 10982-10990
[37] Jia HM, Xu H, Hu Y, Tang YW, Zhang LZ (2007) Electrochemistry Communications 9: 354-360
[38] Z. Zhang, Y. Yuan, Y. Fang, L. Liang, H. Ding, G. Shi, L. Jin (2007) Journal of Electrochemical society 610: 179-185
[39] R.S. Ningthoujam, V. Sudarsan, R.K. Vatsa, R.M. Kadam, Jagannath, A. Guptad (2009) Journal of Alloys and Compounds 486 : 864–870.
[40] Lakshminarayana G, Yang HC, Qiu JR (2009) Journal of Alloys and Compounds 475: 569-576
[41] Yu JG, Wang B (2010) Applied Catalysis B Environmental 94: 295-306
[42] Serpone N, Lawless D, Khairutdinov R (1995) The journal of Physical Chemistry 99:16646-16654
[43] Toyoda T, Hayakawa T, Abe K, Shigenari T, Shen Q (2000) Journal of Luminescence 87: 1237-1239
[44] Huang D, Liao S, Liu J, Dang Z, Petrik L (2006) Journal of Photochemistry and Photobiology A 184: 282-288
[45] Zhao Y, Li CZ, Liu XH , Gu F, Jiang H B, Shao W, Zhang L, He Y (2007) Materials Letters 61: 79-83
[46] Xu J, Li L, Yan Y, Wang H, Wang X, Fu X, Li G (2008) Journal of Colloid and Interface Science 318 : 29-34